Studies on the Kinetic and Chemical Mechanism of Inhibition of Stromelysin by an *N*-(Carboxyalkyl)dipeptide

Maria Izquierdo-Martin,‡ K. T. Chapman,§ W. K. Hagmann,§ and Ross L. Stein*,‡

Department of Enzymology and Medicinal Chemistry Department, Merck Research Laboratories, P.O. Box 2000, Rahway, New Jersey 07065

Received August 31, 1993; Revised Manuscript Received November 15, 1993®

ABSTRACT: We have investigated the inhibition of the human matrix metalloproteinase stromelysin (SLN) by the *N*-(carboxyalkyl)dipeptide Ala[N]hPhe-Leu-anilide and find that it is a competitive, slow-binding inhibitor of this enzyme with $K_i = 3 \times 10^{-8}$ M (pH 6.0, 25 °C). The dependence of k_{obs}, the observed first-order rate constant for the approach to steady state, on Ala[N]hPhe-Leu-anilide concentrations less than 10^{-5} M is linear and suggests a simple, one-step mechanism with $k_{on} = 3.4 \times 10^4$ M^{-1} s^{-1} and $k_{off} = 1.2 \times 10^{-3}$ s^{-1} (pH 6.0, 25 °C). Using rapid kinetic techniques, we extended the concentration range of Ala[N]hPhe-Leu-anilide to 2×10^{-3} M and found that the [Ala[N]hPhe-Leu-anilide] dependence of k_{obs} suggests saturation kinetics with a K_i' near 5×10^{-4} M. Detailed analysis of these data reveal that the dependence of k_{obs} on [Ala[N]hPhe-Leu-anilide] is, in fact, sigmoidal. To probe the chemical mechanism of inhibition, we determined pH and temperature dependencies and solvent deuterium isotope effects. For k_{on}, $\Delta H^{\ddagger} = 12.4$ kcal/mol and $-T\Delta S^{\ddagger} = 6.2$ kcal/mol ($T = 298$ K; $[I]_{steady\text{-}state} = 10^{-6}$ M), while for k_{off}, $\Delta H^{\ddagger} = 12.5$ kcal/mol and $-T\Delta S^{\ddagger} = 8.9$ kcal/mol ($T = 298$ K). pH dependencies of the kinetic parameters for inhibition are complex but reflect greater potency at lower pH and suggest a mechanism involving the same active-site groups that are involved in catalysis. The solvent deuterium isotope effects on k_{on} are large and normal: $k_{on,H_2O}/k_{on,D_2O} = 1.64 \pm 0.07$ at pH 5.5 and 1.81 ± 0.08 at pH 7.5. Together with the pH dependence of inhibition, these values suggest that k_{on} is rate-limited by a process that involves general-acid/general-base catalysis. We suggest that k_{on} is rate-limited by general-acid-catalyzed ligand exchange of inhibitor for the zinc-bound water molecule.

Stromelysin is a member of the family of human matrix metalloproteinases (Matrisian, 1990). The principal members of this family are collagenase, gelatinase, and SLN,[1] and while their role in normal physiology is still unclear, there is strong evidence implicating them in the pathogenesis of osteoarthritis and rheumatoid arthritis. Inhibition of these enzymes is therefore an appealing strategy for pharmacologic intervention in these debilitating diseases.

As part of a program to develop inhibitors of these enzymes, we have examined the mechanism of inhibition of SLN by the *N*-(carboxyalkyl)dipeptide Ala[N]hPhe-Leu-anilide:[2]

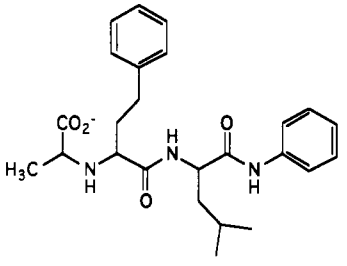

N-(Carboxyalkyl)peptides are a class of metalloproteinase inhibitors that form stable E–I complexes characterized by coordination of the active-site zinc by carbonyl oxygens (Monsingo & Matthews 1984). In these complexes, the zinc-bound water molecule that exists in the active, uninhibited enzyme is absent and has apparently been completely displaced by the inhibitor. The remaining peptide portions of the inhibitor interact with the various substrate subsites of the active site crevice.

In this paper, we report that Ala[N]hPhe-Leu-anilide is a competitive, slow-binding inhibitor of stromelysin. We also define other features of the kinetic mechanism of inhibition of SLN by this compound and go on to probe the chemical mechanism of inhibition through the application of pH and temperature dependencies and solvent deuterium isotope effects.

EXPERIMENTAL PROCEDURES

General. The SLN inhibitor Ala[N]hPhe-Leu-anilide was from a previous study (Chapman et al., 1993). DNP-Arg-Pro-Lys-Pro-Leu-Ala-Phe-TrpNH_2 and Mca-Pro-Leu-Ala-Nva-Dpa-Ala-ArgNH_2 were purchased from Bachem (Philadelphia, PA). Recombinant human prostromelysin (Whitman et al., 1986) was used in all experiments of this paper and was purchased from Celltech Ltd. (Slough, Berkshire, U.K.) at a concentration of 100 μg/mL and a purity of 98%. Trypsin-catalyzed activation of proSLN was according to published procedures (Lark et al., 1990a,b; Teahan et al., 1989). Buffer salts and deuterium oxide were purchased from Sigma.

* To whom correspondence should be addressed at MyoGenics, Inc., 1 Kendall Sq., Building 200, Cambridge, MA 02139.
‡ Department of Enzymology.
§ Medicinal Chemistry Department.
® Abstract published in *Advance ACS Abstracts,* January 15, 1994.

[1] Abbreviations: SLN, stromelysin; DNP, 2,4-dinitrophenyl; Mca, (7-methoxycoumarin-4-yl)acetyl; Dpa, N^3-(2,4-dinitrophenyl)-L-2,3-diaminopropionyl; hPhe, homophenylalanine; Nva, norvaline; FI, fluorescence intensity in arbitrary units; k_{on}, second-order rate constant for association of enzyme and inhibitor; k_{off}, first-order rate constant for dissociation of enzyme–inhibitor complex; $^Dk_{on}$, the solvent deuterium isotope effect on k_{on}.

[2] The nomenclature that we will use for *N*-(carboxyalkyl) inhibitors is exemplified here by Ala[N]hPhe-R, where the N in brackets signifies that the two L-amino acids, Ala and hPhe, "share" a single nitrogen atom.

0006-2960/94/0433-1356$04.50/0

Buffers. For studies of the pH dependence of inhibition, 0.10 M acetate buffer was used for pH 5.0; 0.10 M MES buffers were used for pHs 5.5, 6.0, and 6.5; 0.10 M HEPES buffers were used for pHs 7.0, 7.5, and 8.0; 0.10 M Bicine buffer was used for pH 8.5; and 0.10 M CHES buffers were used for pHs 9.0 and 9.5. In all cases, buffers contained 10 mM $CaCl_2$. Buffers for the solvent isotope effect study was prepared as described previously (Stein et al., 1983, 1987).

Kinetic Experiments: (A) Determination of K_i Values. A stopped-time, single point assay has been developed and described for determining K_i values for the inhibition of SLN and other matrix metalloproteinases (Chapman et al., 1993). Briefly, 1.5 nM SLN is incubated for 4 h with eight concentrations of inhibitor that span a 100-fold concentration range. At the end of this time, the SLN substrate DNP-Arg-Pro-Lys-Pro-Leu-*Ala-Phe*-$TrpNH_2$ is added at a final concentration of 5.7 μM and allowed to react for 18 h. The reaction is then quenched and the unreacted substrate is separated from products by HPLC (Harrison et al., 1992; Teahan et al., 1989). Detection is by absorbance at 215 nm.

In this assay, the low enzyme concentration is used to allow for the analysis of inhibitors with K_i values as low as 0.5 nM. A substrate concentration of 5.7 μM was chosen to ensure subsaturating conditions. A 4-h incubation of enzyme and inhibitor is needed to ensure equilibrium has been reached for slow-binding inhibitors. Finally, the substrate reaction time of 18 h was chosen so that about 70% of the substrate is consumed. This length of time is required since we are at such a low enzyme concentration.

K_i is calculated by nonlinear least-squares fit of the data to the following expression:

$$\frac{\left(-\ln \frac{[S]_t}{[S]_{total}}\right)}{\left(-\ln \frac{[S]_{ti}}{[S]_{total}}\right)} = \frac{k_i}{k} = \frac{1}{1 + \frac{[I]_{total}}{K_i}}$$

where $[S]_t$ and $[S]_{ti}$ are substrate concentrations at time t for the control and inhibited reaction, respectively. The derivation of this expression has been presented (Chapman et al., 1993).

(B) Determination of Inhibition Progress Curves. In these studies, we used a continuous, fluorogenic assay that relies on the ability of DNP to internally quench the fluorescence emission of the tryptophan side chain of the peptide substrate DNP-Arg-Pro-Lys-Pro-Leu-*Ala-Phe*-$TrpNH_2$ (Izquierdo-Martin & Stein, 1992b; Niedzwiecki et al., 1992). The intact peptide shows little fluorescence at 340 nm, since the emitted energy from the indole of Trp is absorbed by the nearly DNP group. When the peptide is hydrolyzed by SLN, the internal quenching of the peptide is released, and an increase in the fluorescence emission at 340 nm is observed. Similar assays have been described for other proteases (Netzel-Arnett et al., 1991; Stack & Gray, 1989).

In a typical kinetic run, 2.94 mL of buffer and 0.020 mL each of substrate and inhibitor in DMSO were added to a 3-mL cuvette and the cuvette was placed in the jacketed cell holder of a Perkin-Elmer 650–40 fluorescence spectrophotometer. Reaction temperature was kept constant to ±0.02 °C. After the reaction solution had reached thermal equilibrium, we initiated the reaction by addition of 0.020 mL of enzyme stock solution. Reaction progress was monitored by the increase in the fluorescence emission at 340 nm (λ_{ex} = 290 nm) that accompanies cleavage of DNP-Arg-Pro-Lys-Pro-Leu-*Ala-Phe*-$TrpNH_2$ at the Ala–Phe bond. For each kinetic run, 1000 data points, corresponding to {time, F} pairs were collected by a NEC Powermate 1 Plus microcomputer interfaced to the fluorescence spectrophotometer.

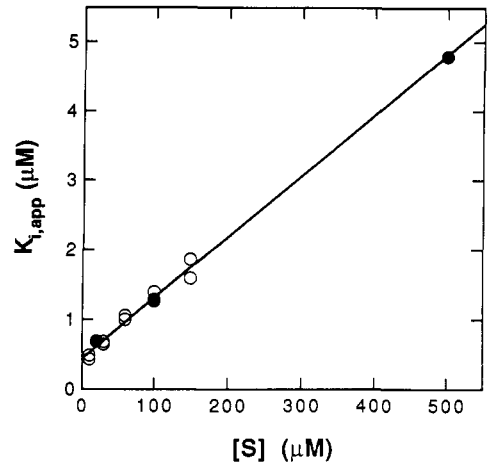

FIGURE 1: Dependence of $K_{i,app}$ on substrate concentration for the inhibition of SLN by Ala[N]hPhe-Leu-anilide. Values of $K_{i,app}$ were determined from steady-state velocities at various concentrations of substrate by two methods: an HPLC-based method (Harrison et al., 1989; Teahan et al., 1989) (filled circles) and a continuous, fluorogenic method (Izquierdo-Martin & Stein, 1992b; Teahan et al., 1989) (empty circles). The substrate in both experiments is DNP-Arg-Pro-Lys-Pro-Leu-Ala-Phe-$TrpNH_2$. The solid line through the combined data points is based on eq 1 and the best-fit parameters K_i = 0.43 ± 0.3 μM and K_m = 49 ± 4 μM.

(C) Stopped-Flow Spectrofluorometry To Determine Kinetics of Inhibition. To determine rate constants for the interaction of SLN with Ala[N]hPhe-Leu-anilide, we performed rapid kinetic experiments on a Hi-Tech stopped-flow spectrofluorometer. A two-syringe mixing configuration was used: syringe A contained 2.6 μM SLN in a pH 6.0 buffer containing 100 mM MES and 10 mM $CaCl_2$, while syringe B contained 31 μM Mca-Pro-Leu-*Ala-Nva*-Dpa-Ala-$ArgNH_2$ and various concentrations of Ala[N]h-Phe-Leu-anilide ($5 \leq [I] \leq 2000$ μM) in a pH 6.0 buffer containing 100 mM MES, 10 mM $CaCl_2$, and 10% DMSO. Mca-Pro-Leu-*Ala-Nva*-Dpa-Ala-$ArgNH_2$ is a fluorogenic substrate for SLN with λ_{ex} = 328 nm and λ_{em} = 393 nm. Similar substrates have been reported for other matrix metalloproteinases (Knight et al., 1992).

RESULTS

Competitive Inhibition of Stromelysin by Ala[N]hPhe-Leu-anilide. In a previous study (Chapman et al., 1993), we reported that the interaction of SLN with Ala[N]hPhe-Leu-anilide is characterized by a K_i value of 0.45 ± 0.05 μM at pH 7.5 and 25 °C. This value was determined at $[S]_0 \ll K_m$ and therefore reflects the true dissociation constant for the SLN–Ala[N]hPhe-Leu-anilide complex. We were curious to know if SLN–Ala[N]hPhe-Leu-anilide is the only complex that accumulates at steady state. To this end, we determined the kinetic mechanism of inhibition by studying the dependence of $K_{i,app}$ on $[S]_0$, where S is DNP-Arg-Pro-Lys-Pro-Leu-*Ala-Phe*-$TrpNH_2$. The results of these experiments are shown in Figure 1 and describe a linear relationship that adheres to the expression of eq 1 for competitive inhibition.

$$K_{i,app} = K_i\left(1 + \frac{[S]_0}{K_m}\right) \quad (1)$$

Least-squares analysis of the data according to eq 1 provides the best-fit values K_i = 0.43 ± 0.3 μM and K_m = 49 ± 4 μM. While the K_i value is identical to the value that we determined

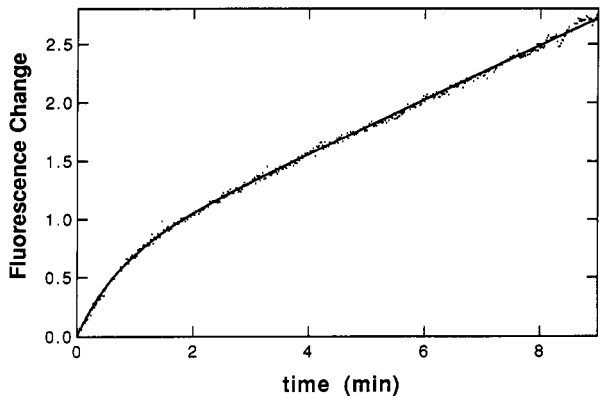

FIGURE 2: Progress curve for the slow-binding inhibition of SLN by Ala[N]hPhe-Leu-anilide. Fluorescence (λ_{ex} = 290 nm, λ_{ex} = 340 nm) was recorded as a function of time for the SLN-catalyzed hydrolysis of DNP-Arg-Pro-Lys-Pro-Leu-*Ala-Phe*-TrpNH$_2$ in the presence of Ala[N]hPhe-Leu-anilide ([E]$_0$ = 0.010 μM, [S]$_0$ = 5.0 μM, [I]$_0$ = 2.0 μM; pH 7.5, 25 °C). The line through the data was drawn using eq 2 and the best-fit parameters v_s = 0.23 ± 0.01 FI/min; v_0 = 1.06 ± 0.05 FI/min, and k_{obs} = 1.29 ± 0.02 min^{-1}.

in independent experiments at low substrate concentration, the K_m value is somewhat less than the value of 82 ± 11 μM that was determined in an independent experiment (data not shown). From this study, it is clear that Ala[N]hPhe-Leu-anilide is a competitive inhibitor of SLN with a K_i value of 0.45 μM.

Time-Dependent Inhibition of Stromelysin by Ala[N]hPhe-Leu-anilide: *(A) 0.5 $\mu M \leq [I] \leq 5$ μM.* In the course of our investigations of the inhibition of SLN by Ala-[N]hPhe-Leu-anilide, we discovered that the compound is a time-dependent inhibitor of SLN. This is illustrated in Figure 2, which contains a reaction progress curve for the SLN-catalyzed hydrolysis of 5 μM DNP-Arg-Pro-Lys-Pro-Leu-*Ala-Phe-TrpNH$_2$* in the presence of 2 μM Ala[N]hPhe-Leu-anilide. This curve is characterized by an initial velocity, v_0, that slowly decays to the final, steady-state velocity, v_s, with first-order rate constant, k_{obs}, and can be fit by nonlinear least-squares to the standard equation for time-dependent or "slow-binding" inhibition (Morrison & Walsh, 1988):

$$[\text{product}] = v_s t + \left[\frac{v_0 - v_s}{k_{obs}}\right][1 - \exp(-k_{obs} t)] \qquad (2)$$

For this progress curve, we determined the following best-fit parameters: v_s = 0.23 ± 0.01 FI/min, v_0 = 1.06 ± 0.05 FI/min, and k_{obs} = 1.29 ± 0.02 min^{-1}. In this and all kinetic experiments reported in this paper, substrate consumption is never greater than 5% of [S]$_0$.

Progress curves similar to the one of Figure 1 were collected at [Ala[N]hPhe-Leu-anilide] ≤ 5 μM and analyzed according to eq 2 to obtain values of k_{obs}. The dependence of k_{obs} on [Ala[N]hPhe-Leu-anilide] is shown in Figure 3 and obeys the expression

$$k_{obs} = k_{on}[I] + k_{off} \qquad (3)$$

This rate equation describes the simple, one-step inhibition mechanism of Scheme 1 in which E combines with I to form E–I with second-order rate constant k_{on} and E–I dissociates with the first-order rate constant k_{off}. In this experiment, we found k_{on} = (1.1 ± 0.1) × 10^4 M^{-1} s^{-1} and k_{off} = (4 ± 2) × 10^{-3} s^{-1} (pH 7.5 and 25 °C). The ratio k_{off}/k_{on} equals 0.36 μM and, as theory predicts, equals the value that has been determined for K_i.

(B) 5 $\mu M \leq [I] \leq 2000$ μM. The results discussed above suggest a one-step mechanism for the interaction of Ala[N]-hPhe-Leu-anilide and SLN. However, a two-step mechanism, such as the one shown in Scheme 2,

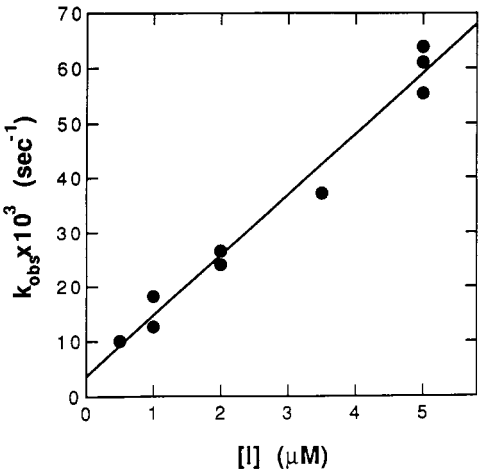

FIGURE 3: Dependence of k_{obs} on low concentrations of Ala[N]hPhe-Leu-anilide. Values of k_{obs} were calculated according to eq 2 for inhibition progress curves at [Ala[N]hPhe-Leu-anilide] ≤ 5 μM ([E]$_0$ = 0.010 μM; [DNP-Arg-Pro-Lys-Pro-Leu-*Ala-Phe*-TrpNH$_2$] = 5 μM ≤ K_m; pH 7.5, 25 °C). The solid line through the data points is based on eq 3 and the best-fit parameters: k_{on} = (1.1 ± 0.1) × 10^4 M^{-1} s^{-1} and k_{off} = (4 ± 2) × 10^{-3} s^{-1}.

Scheme 1: One-Step Kinetic Mechanism for Slow Binding

$$E + I \underset{k_{off}}{\overset{k_{on}}{\rightleftharpoons}} E{:}I$$

Scheme 2: Two-Step Kinetic Mechanism for Slow Binding

$$E + I \underset{K_i'}{\rightleftharpoons} (E{:}I)_1 \underset{k_{-i}}{\overset{k_i}{\rightleftharpoons}} (E{:}I)_2$$

$$k_{obs} = \frac{k_i[I]}{K_i' + [I]} + k_{-i} \qquad (4)$$

$$K_i = K_i'\left(\frac{k_{-i}}{k_i}\right) \qquad (5)$$

would have the appearance of a one-step mechanism if K_i' is much greater than the highest inhibitor concentration, in this case 5 μM (see Figure 3). In the mechanism of Scheme 2, K_i' is the dissociation constant for the initially formed complex, E–I$_1$; k_i is the first-order rate constant for transformation of E–I$_1$ to E–I$_2$; and k_{-i} is the first-order rate constant for transformation of E–I$_2$ back to E–I$_1$. Thus, at low concentrations of inhibitor, the mechanisms of Schemes 1 and 2 are equivalent and we see that

$$k_{on} = \frac{k_i}{K_i'} \qquad (6)$$

and

$$k_{off} = k_{-i} \qquad (7)$$

To probe for the existence of an intermediate along the reaction pathway for the inhibition of SLN by Ala[N]hPhe-Leu-anilide, we needed to determine values of k_{obs} at concentrations of inhibitor that greatly exceed 5 μM. In designing these experiments, it became clear that we would not be able to record inhibition progress curves using conventional kinetic techniques, since k_{obs} increases with increasing concentrations of inhibitor (see eqs 3 and 4). However, using a stopped-flow spectrofluorometer we were able to obtain values of k_{obs} at inhibitor concentrations as high as 2 mM (see Figure 4). These experiments were

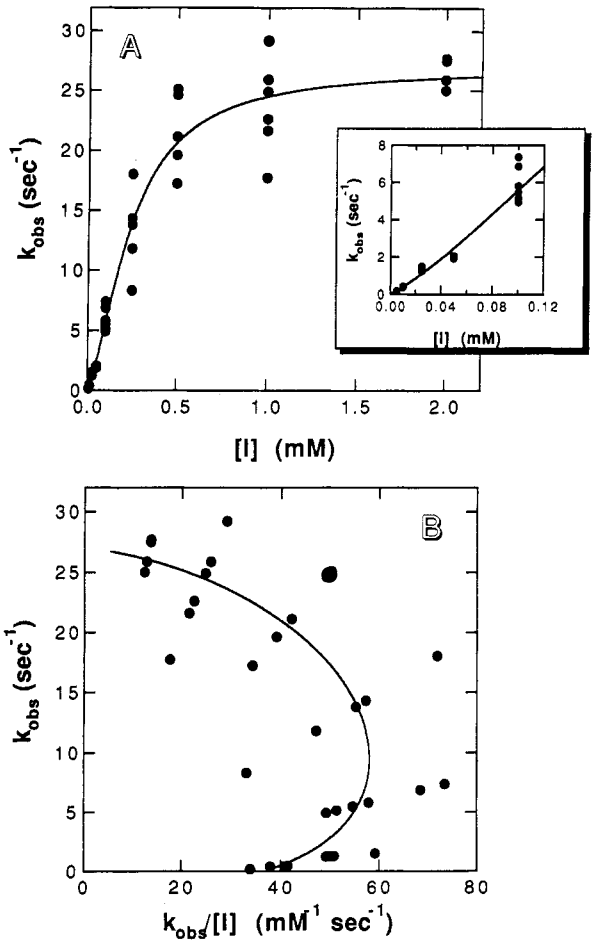

FIGURE 4: Dependence of k_{obs} on high concentrations of Ala[N]-hPhe-Leu-anilide (see text for details of experiment). Final concentrations: [SLN] = 1.3 μM; [Mca-Pro-Leu-*Ala-Nva*-Dpa-Ala-ArgNH$_2$] = 15 μM; 5 μM $\leq$ [Ala[N]hPhe-Leu-anilide] $\leq$ 2000 μM; 100 mM MES and 10 mM $CaCl_2$, pH 6.0 (5% DMSO). (A) Dependence of k_{obs} on [Ala[N]hPhe-Leu-anilide]. Solid line through the data points is drawn according to the sigmoidal expression of eq 10 and the best-fit parameters k_i = 26 $\pm$ 1 s^{-1}, K_i' = 660 $\pm$ 290 μM, and K_{ii}' = 130 $\pm$ 110 mM. The inset is an expansion of a portion of the main figure and is included to emphasize the sigmoidal nature of the data. (B) Eadie–Hoffstee plot of the data of panel A.

conducted with $[E]_0$ = 1.3 μM and $[S]_0$ = 15 μM (pH 6.0, 26 °C) where the substrate is the new fluorogenic peptide Mca-Pro-Leu-*Ala-Nva*-Dpa-Ala-ArgNH$_2$ (λ_{ex} = 328 nm, λ_{em} = 393 nm; k_c/K_m = 31 000 M^{-1} s^{-1}, pH 6.0, 25 °C). In all case, since $[I]_0 \gg K_i$, the progress curves were strictly first-order with $v_s \approx 0$.

Inspection of the results of Figure 4 reveals two significant findings: (i) At concentrations of Ala[N]hPhe-Leu-anilide greater than 0.5 mM, k_{obs} becomes independent of inhibitor concentration and equal to about 26 s^{-1}. Saturation kinetics such as this indicates the existence of at least one intermediate along the reaction pathway to the stable enzyme–inhibitor complex that accumulates in the steady state. (ii) The dependence of k_{obs} on [Ala[N]hPhe-Leu-anilide] is sigmoidal and not hyperbolic as predicted by the mechanism of Scheme 2. This requires us to consider more complex mechanisms and high-order, phenomenologic kinetic equations of the general form that has been described by Bardsley (Bardsley et al., 1980) for enzyme catalysis:

$$k_{obs} = \frac{\alpha_1[I] + \alpha_2[I]^2 + ... + \alpha_n[I]^n}{\beta_0 + \beta_1[I] + \beta_2[I]^2 + ... + \beta_n[I]^n} \quad (8)$$

Scheme 3: Mechanistic Proposal for the Inhibition of Stromelysin by Ala[N]hPhe-Leu-anilide

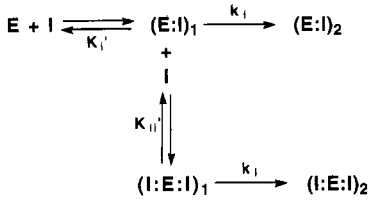

The data of Figure 4 are consistent with a form of eq 8 where n = 2:

$$k_{obs} = \frac{\alpha_1[I] + \alpha_2[I]^2}{\beta_0 + \beta_1[I] + \beta_2[I]^2} \quad (9)$$

Equation 9 can be rearranged to produce the more familiar-looking expression[3]

$$k_{obs} = \frac{k_i[I]\left(1 + \frac{[I]}{K_{ii}'}\right)}{K_i' + [I]\left(1 + \frac{[I]}{K_{ii}'}\right)} \quad (10)$$

This equation describes the mechanism of Scheme 3 in which a second molecule of inhibitor can bind to $(E–I)_1$ to form $(I–E–I)_1$. Both of these intermediary complexes can then undergo transformation to their respective final, steady-state complexes, $(E–I)_2$ and $(I–E–I)_2$.

According to Scheme 3, a sigmoidal dependence of k_{obs} on [I] will only be observed in situations in which K_{ii}' is less than K_i'. This is confirmed by nonlinear least-squares analysis of the data of Figure 4A to eq 10, where we find k_i = 26 $\pm$ 1 s^{-1}, K_i' = 660 $\pm$ 290 μM, and K_{ii}' = 130 $\pm$ 110 μM.

A question that we need to consider at this point is, Do we actually need sigmoid kinetics to explain the data of Figure 4A? We believe that that the answer to this question is yes, and we support it as follows: (1) The data of Figure 4A are replotted as k_{obs} vs $[I]/k_{obs}$ in Figure 4B. Even casual inspection of this plot reveals obvious nonlinearity. The curve doubles back on itself, which is a signature for sigmoidal kinetics. (2) Table 1 summarizes best-fit parameters from the results of nonlinear regression analysis of the data of Figure 4A according to the mechanisms of Schemes 2 and 3 (eqs 4 and 10, respectively). The sum of the squares of residuals is much lower for the fit to eq 10 than to eq 4, indicating that the data set is more consistent with Scheme 3 than Scheme 2. (3) Finally, the data of Figure 2 that were collected at low concentrations of Ala[N]hPhe-Leu-anilide are more consistent with Scheme 3 than with Scheme 2 (see Table 1). We see that at low concentrations of inhibitor eq 10 reduces to

$$k_{obs} = \frac{k_i}{K_i'}[I] \quad (11)$$

From this analysis, k_i/K_i' can be calculated to be 40 000 M^{-1} s^{-1}, which is identical to the value of k_{on} obtained by conventional kinetic methods at pH 6.0 (see below and Table 1).

pH Dependence of the Slow-Binding Inhibition of Stromelysin by Ala[N]hPhe-Leu-anilide. To probe the mechanism of the slow-binding inhibition of SLN by Ala[N]hPhe-Leu-anilide, we determined the pH dependence of K_{ass} (= $1/K_i$),

[3] Note that k_{-i} is not included in either eq 10 or the mechanism of Scheme 3. This is because k_{-i} ($\approx$ 0.001 s^{-1}) is so much less than any k_{obs} value of Figure 4 (0.17 s^{-1} $\leq$ k_{obs} $\leq$ 25 s^{-1}).

Table 1: Kinetic Analysis of the Dependence of k_{obs} on Inhibitor Concentration for the Slow-Binding Inhibition of SLN by Ala[N]hPhe-Leu-analide[a]

mechanism	[Ala[N]hPhe-Leu-anilide] range (μM)	k_i (s^{-1})	K_i' (μM)	K_{ii}' (μM)	k_i/K_i' (M^{-1} sec^{-1})	Σ(resid)^2
Scheme 3	5–2000	26 ± 1	660 ± 290	130 ± 110	40 000	175
Scheme 2	5–2000	32 ± 2	360 ± 50		89 000	286
Scheme 1	0.5–5.0				34 000	

[a] pH 6.0, 25 °C.

k_{on}, and k_{off}. We obtained these constants at various pH values according to the method described below.

From our analyses of inhibition progress curves that were determined at [S] $\ll K_m$ and [Ala[N]hPhe-Leu-anilide] ≤ 5 μM (see above), we know the following: (i) v_0 is independent of inhibitor concentration and equals the control velocity determined in the absence of inhibitor, (ii) v_s depends on inhibitor concentration according to

$$v_s = \frac{v_0}{1 + \frac{[I]}{K_i}} \quad (12)$$

and (iii) k_{obs} is linearly dependent on inhibitor concentration. As we described above, these observations support the simple mechanism of Scheme 1, according to which the linear dependence of k_{obs} on inhibitor concentration is described by eq 3 and the inhibition constant, K_i, is given by the ratio k_{off}/k_{on}. These kinetic relationships allow us to calculate K_i, k_{on}, and k_{off} according to the following equations:

$$K_i = \frac{[I]}{\frac{v_0}{v_s} - 1} \quad (13)$$

$$k_{on} = \frac{k_{obs}}{[I] + K_i} \quad (14)$$

$$k_{off} = k_{on}K_i \quad (15)$$

Thus a single progress curve contains enough information to calculate K_i, k_{on}, and k_{off} at any pH value or other set of experimental conditions that is varied (e.g., isotopic composition of solvent water or temperature).

In practice, after a progress curve is obtained, best-fit values for v_0, v_s, and k_{obs} are determined, and K_i is calculated from eq 13 and then used together with eq 14 to calculate k_{on}. Finally, k_{off} is estimated as $k_{on}K_i$. Replicate determinations at given pH provide means and standard deviations that are never greater than 10%.

Using this general method, values of K_{ass}, k_{on}, and k_{off} were determined at pH values that ranged from 5.0 to 9.5. These values are summarized in Table 2 and displayed graphically in Figures 5–7. While the pH dependence of K_{ass} has a simple bell shape (Figure 5), the pH dependencies of k_{on} and k_{off} are more complex. Viewed broadly, however, we see that inhibitory potency decreases with increasing pH. This is reflected in decreasing values of K_{ass} and k_{on} and increasing values of k_{off} with increasing pH (see below). A detailed, quantitative analysis of these results is described below and consists of individual analyses of the three dependencies followed by an attempt to incorporate them into an overall mechanism for the pH dependence of inhibition of SLN by Ala[N]hPhe-Leu-anilide.

pH Dependence of K_{ass}. The dependence of log (K_{ass}) on pH from three independent experiments is shown in Figure 5. We see that inhibitor potency increases with decreasing pH to a maximum at pH 6.0 and then decreases as pH decreases further. The simplest kinetic mechanism that can account for the data is shown in Scheme 4.[4] The simplicity of this mechanism is deceptive and, as we see below, results only because of cancellation of compensating terms in the pH dependencies of k_{on} and k_{off}.

Table 2: pH Dependence of the Kinetics of Inhibition of Stromelysin by Ala[N]hPhe-Leu-anilide[a,b]

pH	K_i (μM)	K_{ass} (μM^{-1})	k_{on} (M^{-1} s^{-1})	$10^4 k_{off}$ (s^{-1})
5.0	0.078	15	48 000	32
5.5	0.027	37	41 000	11
6.0	0.030	27	34 000	12
6.5	0.043	30	23 000	8
7.0	0.12	8.3	19 000	23
7.5	0.33	3.0	11 000	36
8.0	0.53	1.7	7900	47
8.5	2.8	0.36	3300	92
9.5	26	0.038		

[a] 25 °C. [b] These values are the of means of replicate determinations at each pH. Relative standard deviations are less than 15% in all cases.

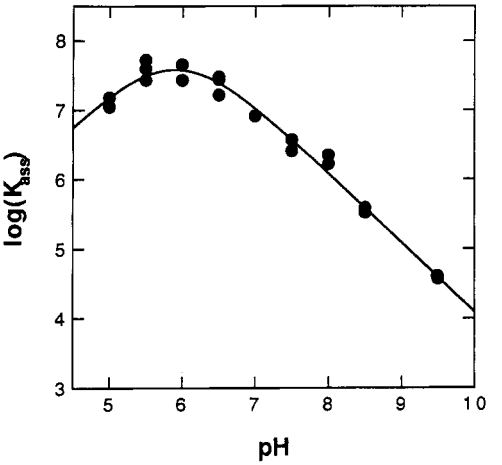

FIGURE 5: pH dependence of K_{ass} for the inhibition of SLN by Ala-[N]hPhe-Leu-anilide. Values of K_{ass} were determined as described in the text as a function of pH. Data points represent the combined results of three independent experiments. The line through the data points was drawn using eq 16 and the following parameters: $(K_i)_{limit}$ = 13 ± 4 nM; $pK_{a,E3}$ = 5.6 ± 0.3; $pK_{a,E2}$ = 6.2 ± 0.2.

Scheme 4: pH Dependence of K_{ass} for the Inhibition of SLN by L696,418

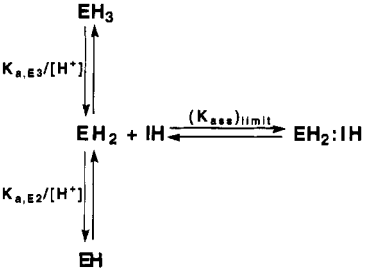

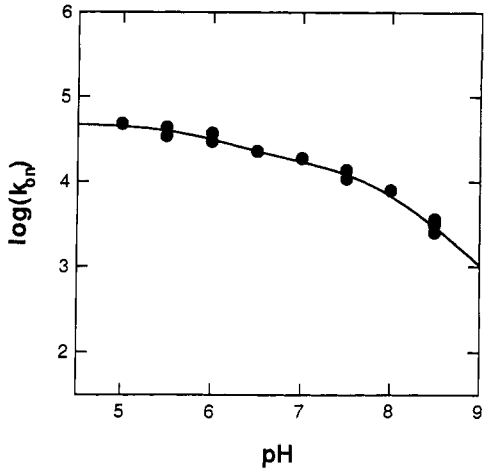

FIGURE 6: pH dependence of k_{on} for the inhibition of SLN by Ala-[N]hPhe-Leu-anilide. Values of k_{on} were determined as described in the text as a function of pH. Data points represent the combined results of two independent experiments. The line through the data points was drawn using eq 17 and the following parameters: $k_{on,2}$ = 48 ± 7 mM^{-1} s^{-1}, $k_{on,1}$ = 17 ● 4 mM^{-1} s^{-1}, $pK_{a,E2}$ = 6.0 ± 0.3, and $pK_{a,I}$ = 7.8 ± 0.1.

The kinetic expression for the mechanism of Scheme 4 is

$$K_{ass} = \frac{(K_{ass})_{limit}}{\frac{[H^+]}{K_{aE3}} + 1 + \frac{K_{aE2}}{[H^+]}} \quad (16)$$

When the data set of Figure 5 is fit to this equation, the following best-fit parameters are found: $(K_i)_{limit}$ = 13 ± 4 nM, $pK_{a,E3}$ = 5.6 ± 0.3, and $pK_{a,E2}$ = 6.2 ± 0.2. These values and eq 16 were used to draw the solid line through the data points of Figure 5. Significantly, $pK_{a,E3}$ and $pK_{a,E2}$ are identical to pK_a values that are important for catalysis by SLN (Harrison et al., 1992; Stein & Izquierdo-Martin, 1993).

pH Dependence of k_{on}. Figure 6 shows the pH dependence of k_{on} for the binding of Ala[N]hPhe-Leu-anilide to SLN. Unlike the bell-shaped pH dependence of K_{ass}, the pH dependence of k_{on} has a plateau of maximum activity at acid pH. Close inspection of the data in Table 2 and Figure 6 reveals a shallow dependence of k_{on} on pH; that is, as $[H^+]$ decreases by over 4 orders of magnitude, k_{on} decreases by only a factor of 15. The simplest model that can account for our data is shown in Scheme 5 and involves two pH-dependent pathways for the association of enzyme and inhibitor.

Scheme 5: pH Dependence of k_{on} for the Inhibition of Stromelysin by Ala[N]hPhe-Leu-anilide

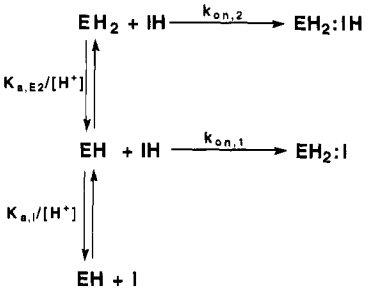

The best-fit parameters for the fit of the data to the rate equation for this model

$$k_{on} = \frac{k_{on2}}{1 + \frac{K_{aE2}}{[H^+]}} + \frac{k_{on1}}{\frac{[H^+]}{K_{aI}} + 1} \quad (17)$$

are $k_{on,2}$ = 48 ± 7 mM^{-1} s^{-1}, $k_{on,1}$ = 17 ± 4 mM^{-1} s^{-1}, $pK_{a,E2}$ = 6.0 ± 0.3, and $pK_{a,I}$ = 7.8 ± 0.1.

In this model, the pK_a of 6.0 is assigned to an enzyme active-site residue. This is presumably the same residue that titrates K_{ass} ($K_{a,E2}$ above) and k_c/K_m (Harrison et al., 1992; Stein & Izquierdo-Martin, 1993) with pK_a values of 6.2. The fact that the pH dependence of k_{on} shows no inflection with a pK_a of 5.6 indicates that $k_{on,3}$ must be approximately equal to $k_{on,2}$. A more complete mechanism that incorporates this feature is given below.

A pK_a of 7.8 has not been observed before for either SLN catalysis or inhibition. However, this value is nearly identical to the dissociation constant of 7.4 ± 0.3 that was determined for the ionization of the secondary amine of Ala[N]hPhe-Leu-anilide (data not shown):

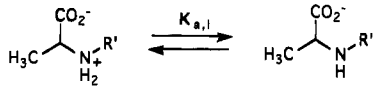

This is incorporated into the mechanism of Scheme 5, which states that only the protonated form of the Ala[N]hPhe-Leu-anilide can bind to SLN.[5]

pH Dependence of k_{off}. The dependence of k_{off} on pH is shown in Figure 7. The simplest mechanism that can account for the complex shape of this curve is shown in Scheme 6. This mechanism states that each of the three ionized forms of the enzyme–inhibitor complex can dissociate to free enzyme and inhibitor. Qualitatively, the results of Figure 7 are consistent with the kinetic situation in which $k_{off,3} \approx k_{off,1} \gg k_{off,2}$.

The rate equation that describes the mechanism of Scheme 6 is

$$k_{off} = \frac{k_{off3}}{1 + \frac{K_{aE3'}}{[H^+]} + \frac{K_{aE3'}K_{aE2'}}{[H^+]^2}} + \frac{k_{off2}}{\frac{K_{aE3'}}{[H^+]} + 1 + \frac{K_{aE2'}}{[H^+]}} + \frac{k_{off}}{\frac{[H^+]^2}{K_{aE3'}K_{aE2'}} + \frac{[H^+]}{K_{aE2'}} + 1} \quad (18)$$

The data set could not be fit to eq 18 due to nonconvergence.

[4] The nomenclature that we use for dissociation constants and kinetic parameters is based on mechanistic considerations for both SLN catalysis and inhibition. Kinetic experiments for substrate hydrolysis (Harrison et al., 1992; Stein & Izquierdo-Martin, 1993) are consistent with no less than three active-site ionizations:

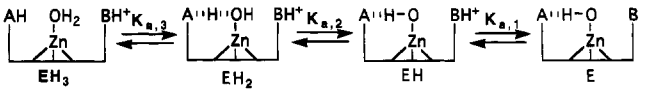

According to this mechanism, the active site of SLN contains a zinc-bound water molecule as well as two titratable, catalytically-important amino acid residues, A and B. At the present time, the identity of A and B is unknown. Although four protons are shown in our depiction of the active site at low pH, only three will ultimately be titratable in the pH range of our experiments. These titrations are governed by the three K_a values shown in the scheme. This forms the basis of our nomenclature. For example, the proton dissociation of EH_3 to EH_2 is governed by $K_{a,3}$, while the association of inhibitor with EH_2 to form EH_2–I is governed by $K_{ass,2}$. Proton dissociation constants that have prime superscripts refer to enzyme–inhibitor complexes. Thus, $K_{a,3}'$ governs the dissociation of EH_3–I to EH_2–I.

[5] In this scheme, EH reacts with IH to produce EH_2–I and not EH–IH. The necessity of this proton switch from inhibitor to enzyme will be described in the Discussion section when a proposal for the chemical mechanism of inhibition is presented.

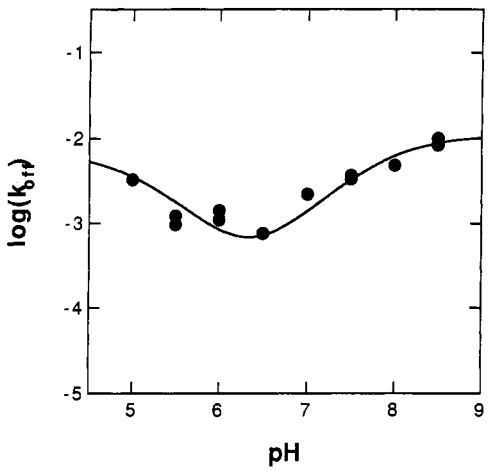

FIGURE 7: pH dependence of k_{off} for the inhibition of SLN by Ala-[N]hPhe-Leu-anilide. Values of k_{off} were determined as described in the text as a function of pH. Filled and empty circles correspond to two independent experiments. The line through the data points was drawn using eq 18 and the following parameters: $k_{off,3}$ = (6.8 ± 7.6) × 10^{-3} s^{-1}, $k_{off,2}$ = 0.1 × 10^{-3} s^{-1}, $k_{off,1}$ = (11 ± 1) × 10^{-3} s^{-1}, p$K_{a,E3'}$ = 4.9 ± 0.7, and p$K_{a,E2'}$ = 7.9 ± 0.1.

Scheme 6: pH Dependence of k_{off} for the Interaction of SLN and Ala[N]hPhe-Leu-anilide

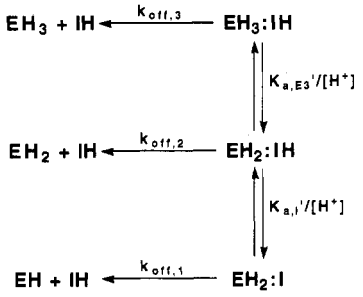

Scheme 7: pH Dependence of the Inhibition of SLN by Ala[N]hPhe-Leu-anilide

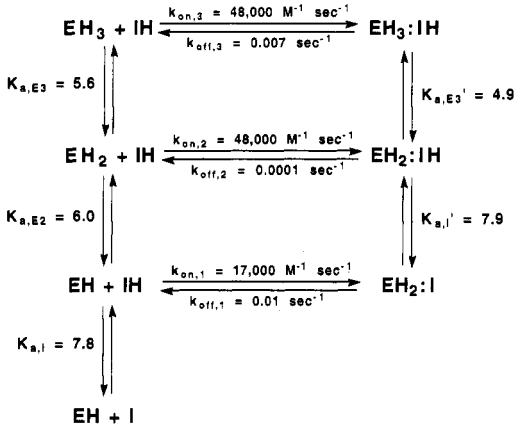

This indicates that there is no unique set of kinetic parameters that can define our data for the pH dependence of k_{off}. However, if $k_{off,2}$ is constrained to a value that is much less than $k_{off,3}$ and $k_{off,1}$, then the following parameter estimates are found: $k_{off,3}$ = (6.8 ± 0.6) × 10^{-3} s^{-1}, $k_{off,1}$ = (11 ± 1) × 10^{-3} s^{-1}, p$K_{a,E3'}$ = 4.9 ± 0.7, and p$K_{a,E2'}$ = 7.9 ± 0.1. These parameters, along with a value of 0.1 × 10^{-3} s^{-1} for $k_{off,3}$ were used to draw the solid line in Figure 7.

Scheme 7 summarizes our analysis of the pH dependence of inhibition of SLN by Ala[N]hPhe-Leu-anilide. A unique feature of this mechanism is that although the ionization state of the inhibitor is not important in determining K_i, it is critically important in determining the magnitude of k_{on} and k_{off}. The insensitivity of K_i to this ionization results from a cancellation of terms in k_{on} and k_{off} that contain $K_{a,I}$.

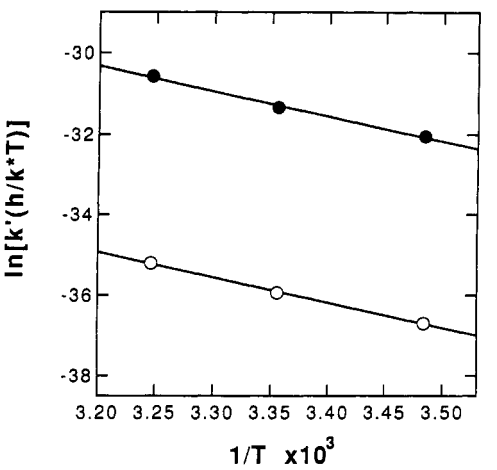

FIGURE 8: Temperature dependencies of k_{on} and k_{off} for the inhibition of SLN by Ala[N]hPhe-Leu-anilide. Eyring plots were constructed from values of k_{off} (open circles) and k_{on}' (closed circles) where k_{on}' = $k_{on}[I]_{standard\text{-}state}$ = $k_{on}(10^{-6}$ M). Reactions were conducted in a pH 5.5 buffer containing 100 mM MS and 10 mM $CaCl_2$.

Table 3: Thermodynamic and Activation Parameters for the Inhibition of Stromelysin by Ala[N]hPhe-Leu-anilide[a,b]

parameter	ΔH (kcal/mol)	ΔS (entropy units)	$-T\Delta S^c$ (kcal/mol)
k_{on} [d]	12.4 ± 0.7	−21 ± 2	6.2 ± 0.8
k_{off}	12.5 ± 0.4	−30 ± 1	8.9 ± 0.4
K_{ass}	0.0 ± 0.4	9.3 ± 1.3	2.8 ± 0.4

[a] 100 mM MES and 10 mM $CaCl_2$, pH 5.5. [b] For k_{on} and k_{off}, activation parameters were calculated from Eyring plots, while for K_{ass}, thermodynamic parameters were calculated from a van't Hoff. [c] T = 298 K. [d] k_{on}' = $k_{on}[I]_{standard\text{-}state}$ = $k_{on}(10^{-6}$ M).

Solvent Deuterium Isotope Effects. To probe the transition-state structure for the association of Ala[N]hPhe-Leu-anilide with SLN, we determined $^Dk_{on}$ values at pH 5.5 and 7.5 and their pD equivalents. In these experiments, [E] = 10 nM, [S] = 5 μM, and [I] = 1 and 5 μM for pH 5.5 and 7.5, respectively. Values of k_{obs,H_2O} and k_{obs,D_2O} were determined from analyses of progress curves for the hydrolysis of DNP-Arg-Pro-Lys-Pro-Leu-*Ala-Phe*-TrpNH$_2$ in the presence of high concentrations of Ala[N]hPhe-Leu-anilide, where $k_{on}[I] \gg k_{off}$. Therefore, $k_{obs}/[I] = k_{on}$ and $^Dk_{obs} = {}^Dk_{on}$. At pH values of 5.5 and 7.5, we determined $^Dk_{on}$ values of 1.64 ± 0.07 and 1.81 ± 0.08, respectively. These values are the means and standard deviations of six determinations at each pH.

Temperature Dependence of Inhibition. Values of k_{on} and k_{off} were determined as outlined above at 14, 25, and 45 °C (pH 5.5). The results are expressed in Figure 8 as Eyring plots of ln $[k'(h/kT)]$ vs $1/T$, where h is Planck's constant, k^* is Boltzmann's constant, T is expressed in degrees Kelvin, and k' is either k_{off} or k_{on}', a pseudo-first-order rate constant obtained by multiplying k_{on} by a standard-state inhibitor concentration of 10^{-6} M. Both plots are linear and allow us to calculate the enthalpy and entropy of activation from

$$\ln\left[k'\left(\frac{h}{k^*T}\right)\right] = -\frac{\Delta H^\ddagger}{R}\frac{1}{T} + \frac{\Delta S^\ddagger}{R} \qquad (19)$$

These values are summarized in Table 3. The van't Hoff plot of K_{ass}' vs $1/T$, where K_{ass}' = $K_{ass}[I]_{standard\text{-}state}$ = $K_{ass}(10^{-6}$ M), is also linear (data not shown) and gave us the thermodynamic parameters that are summarized in Table 3.

DISCUSSION

In a previous publication (Chapman et al., 1993), we reported on the inhibition of SLN by a series of *N*-(carboxyalkyl)peptides. To understand how these compounds inhibit SLN, we performed the experiments described herein on the prototype, Ala[N]hPhe-Leu-anilide. The results of these experiments and their mechanistic implications are discussed below.

Kinetic Mechanism of Inhibition of Stromelysin by Ala[N]-hPhe-Leu-anilide. The results of this paper demonstrate that Ala[N]hPhe-Leu-anilide is a competitive, time-dependent inhibitor of SLN with K_i = 30 nM, k_{on} = 34 mM^{-1} s^{-1}, and k_{off} = 1.2 × 10^{-3} (pH 6.0, 25 °C). An unexpected and intriguing result is the sigmoidal dependence of k_{obs} on [Ala[N]hPhe-Leu-anilide] that we observed in our rapid kinetics experiment (Figure 4). At low concentration of inhibitor, the dependence of k_{obs} on [Ala[N]hPhe-Leu-anilide] is linear with a slope of 40 mM^{-1} s^{-1} (Table 1), which is essentially identical to the result that we obtained in this concentration range using conventional kinetic techniques. As the concentration of Ala[N]hPhe-Leu-anilide increases above about 10 μM, k_{obs} increases according to the second-order expressions of eqs 9 and 10. At high concentrations of Ala[N]hPhe-Leu-anilide, k_{obs} plateaus at a value of 26 s^{-1}. The underlying molecular mechanism that gives rise to this sigmoidal behavior is unclear. While the simplest mechanism is the one shown in Scheme 3 involving the binding of two molecules of inhibitor to SLN, other kinetics-based models are also possible (Bardsley et al., 1980).

Even though the kinetics of inhibition are complex, they clearly reveal a mechanism that involves at least one intermediate on the reaction pathway to the final, enzyme–inhibitor complex that accumulates in the steady state. Our analysis reveals that the dissociation constant for this complex is around 0.5 mM. This reflects relatively weak interactions with the enzyme and suggests that the complex is a simple Michaelis-like encounter complex. This complex is stabilized by a factor of 2 × 10^4 ($=k_i/k_{-i}$) or 6 kcal/mol when it is transformed to the final complex that accumulates in the steady state. Transformation to the final complex is governed by a first-order rate constant, k_i, of 26 s^{-1}, and as we discuss further below, may reflect ligand exchange on zinc of inhibitor carboxylate for water.

Another example of time-dependent inhibition of a metalloproteinase by an *N*-(carboxyalkyl)dipeptide is the inhibition of angiotensin-converting enzyme by hPhe[N]Ala-Pro ($K_i \approx 10^{-10}$ nM) (Shapiro & Riordan, 1984). The inhibition mechanism of this interaction also involves an intermediary complex, but here K_i' is about 10^{-8} M and reflects much stronger initial interactions than we see for SLN and Ala[N]hPhe-Leu-anilide.

pH Dependence of the Inhibition of Stromelysin by Ala[N]-hPhe-Leu-anilide. Our analysis of the pH dependence of inhibition of SLN by Ala[N]hPhe-Leu-anilide led to the kinetic mechanism and rate constant assignments of Scheme 7. What remains to be done is to translate this into a rational chemical mechanism of inhibition. Since we do not know the identity of the active-site residues, this by necessity will be speculation, but speculation based on other pH dependencies for SLN and analogy to TLN for which there is both structural and kinetic information. The mechanism that we propose is shown in Scheme 8. We start with the association of EH_2 and IH to form EH_2–IH. This reaction occurs with expulsion of the active-site water molecule and bidentate coordination of the active-site zinc with the carboxylate moiety of the inhibitor.

Scheme 8: Mechanism for the pH Dependence of Inhibition of SLN by Ala[N]hPhe-Leu-anilide

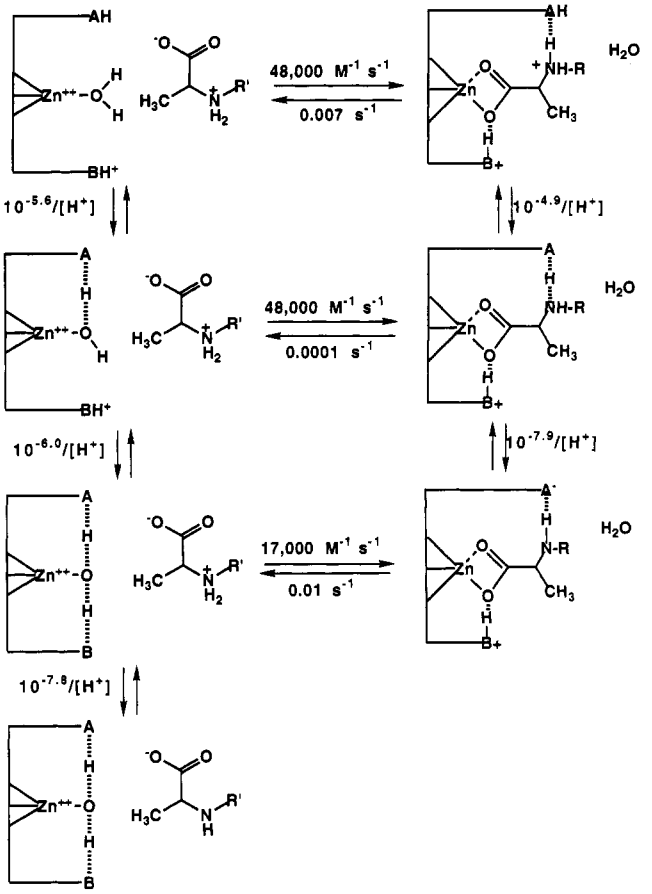

Two hydrogen bonds are also present in EH_2–IH, one between BH^+ and a carboxylate oxygen and the other between A^- and the protonated nitrogen of the inhibitor. Presumably, these hydrogen bonds play some role in stabilizing EH_2–IH. This could be either direct stabilization, if these hydrogen bonds are stronger than those involved in solvating EH_2 and IH in solution, or indirect stabilization, if the hydrogen bonds help to orient the inhibitor within the active site for optimal interaction with the enzyme. Bidentate coordination of the zinc and this pattern of hydrogen-bonding interactions are similar to what has been observed at the active site of TLN when it is complexed with the inhibitor hPhe[N]Leu-Trp (Monsingo & Matthews, 1984).

As the pH is lowered, EH_2–IH is protonated with a pK_a of 4.9 to form EH_3–IH. In this latter complex, A^- has become protonated to form AH. Since AH is a weaker hydrogen-bond acceptor than its conjugate base, A^-, it will not interact as strongly with the protonated amine of the inhibitor, thereby destabilizing EH_3–IH relative to EH_2–IH. Loss of this stabilizing interaction in EH_3–IH accounts for the increase in k_{off}.

Again starting with EH_2–IH, we see that as the pH is raised, the enzyme-bound inhibitor of EH_2–IH ionizes with a pK_a of 7.9 to form EH_2–I. The inhibitor in this complex is a weaker hydrogen-bond donor than it was in EH_2–IH. This destabilizes EH_3–IH relative to EH_2–IH and, consequently, k_{off} increases.

An interesting feature of this mechanism is that the ionizing group, Zn^{2+}-OH_2, that appears in free enzyme does not exist in any of the enzyme–inhibitor complexes. Thus, when a proton dissociates from EH_2–IH, the proton dissociates from the inhibitor portion of the complex to produce EH_2–I. Also, when the complex EH_2–I dissociates to free enzyme and

inhibitor, EH and IH are produced. This requires a proton switch from enzyme to inhibitor and is necessary to account for the observed pK_a of 6 in the uncomplexed state of enzyme and inhibitor.

Finally, as the pH raises further, free inhibitor ionizes with a pK_a value of 7.8. This results in $k_{on,obs}$ going to zero and indicates that only the protonated form of the inhibitor can interact with enzyme.

The pH dependence of inhibition of SLN by Ala[N]hPhe-Leu-anilide is similar to the pH dependence that we have reported for the inhibition of SLN by a peptide phosphonamidate (Izquierdo-Martin & Stein, 1993). In both cases, we find that (i) potency of inhibition increases with decreasing pH, (ii) multiple forms of SLN that differ by their ionization state can bind inhibitor, and (iii) pK_a values that are extracted from the analysis of the inhibition data are identical to pK_a values extracted from analysis of the pH dependence of k_c/K_m for substrate hydrolysis (Harrison et al., 1992; Stein & Izquierdo-Martin, 1993). A mechanism similar to what we proposed for the inhibition of SLN by Ala[N]hPhe-Leu-anilide was proposed to account for SLN's interaction with the phosphonamidate. The generality of this mechanism is also supported by the pH dependence of inhibition of SLN by other *N*-(carboxyalkyl)peptides and phosphorus-containing inhibitors (unpublished data of the authors).

Solvent Deuterium Isotope Effects for the Association of Stromelysin with Ala[N]hPhe-Leu-anilide. To explore transition-state structural features for the association of SLN with Ala[N]hPhe-Leu-anilide, we determined the solvent deuterium isotope effect for k_{on}. Values of $^Dk_{on}$ determined at pH 5.5 and 7.5 are similar and equal, 1.6 ± 0.1 and 1.8 ± 0.1, respectively. In the discussion that follows, we will use the average, pH-independent value of 1.7.

$^Dk_{on}$ can be interpreted in terms of the general expression

$$^Dk_{on} = Z^{-1}\frac{\Pi\Phi_{reactant}}{\Pi\Phi_{\neq}} \quad (20)$$

which expresses $^Dk_{on}$ as the ratio of products of reactant state and transition-state fractionation factors (Quinn & Sutton, 1991) multiplied by a term, Z, that reflects medium effects (Kurz et al., 1992; Stein, 1985a,b; Stein et al., 1983). To understand the structure of the transition state, we must calculate $\Pi\Phi_{\neq}$ from this expression.

For the reaction under consideration here, we first expand eq 20 to

$$^Dk_{on} = Z^{-1}\frac{(\Phi_{Zn\text{-}OH_2})^2[\Pi\Phi_{inhibitor}][\Pi\Phi_{stromelysin}]}{\Pi\Phi_{\neq}} \quad (21)$$

where $\Phi_{Zn\text{-}OH_2}$ is the fractionation factor for one of the two hydrogens of the zinc-bound water molecule and $\Pi\Phi_{inhibitor}$ and $\Pi\Phi_{stromelysin}$ are the products of fractionation factors for the inhibitor and enzyme, respectively.

Z is the product of many small fractionation factors that originate from the solvent reorganization that accompanies binding of substrate or inhibitor (Schowen & Schowen, 1982; Stein & Matta, 1985; Venkatasubban & Schowen, 1985) and is similar in magnitude to solvent isotope effects on dissociation constants for E–S or E–I complexes when the processes governed by K_s or K_i do not contain chemical steps (Kurz et al., 1992; Stein, 1985a,b; Stein et al., 1983). We, unfortunately, do not know the magnitude of Z for the interaction of SLN and Ala[N]hPhe-Leu-anilide. While ^DK_m for the SLN-catalyzed hydrolysis of Arg-Pro-Lys-Pro-Gln-*Gln-Phe*-Phe-Gly-Leu-$NleNH_2$ is 2.0 ± 0.2 (Harrison et al., 1992), K_m for this reaction is thought to reflect chemistry and thus is not the dissociation constant for E–S. Since values of Z that are larger than 1.0 will only serve to enlarge the observed isotope effect, we will take the conservative position and, in the arguments that follow, assume that Z is unity.

Chart 1: Proposed Transition-State Structure for the Association of SLN with Ala[N]hPhe-Leu-anilide

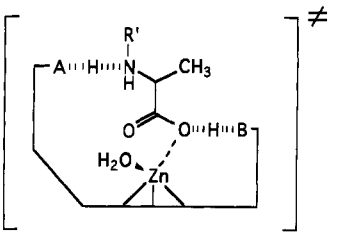

We can now calculate a value for $\Pi\Phi_{\neq}$. If we make the reasonable assumptions that the fractionation factors for the inhibitor and enzyme are unity (Quinn & Sutton, 1991; Venkatasubban & Schowen, 1985) and set $\Phi_{Zn\text{-}OH_2}$ equal to 0.85 (Izquierdo-Martin & Stein, 1992a,b; Kassebaum & Silverman, 1989; Schmidt et al., 1979), we can use eq 21 and $^Dk_{on}$ = 1.7 to calculate a value for $\Pi\Phi_{\neq}$ of 0.42. The inverse of this value is 2.4 and reflects the transition-state contribution to the overall isotope effect. We see then that the observed isotope effect of 1.7 is the transition-state contribution of 2.4 offset by a ground-state contribution of 0.74 (=0.85^2). Note that the transition-state contribution to the isotope effect will increase as Z increases, since $(\Pi\Phi_{\neq})^{-1} = Z^Dk_{on}(\Pi\Phi_{reactant})^{-1} = Z(2.4)$.

The normal isotope effect on k_{on} of 1.7 suggests a transition-state structure that involves proton bridging of the sort observed in general-acid/general-base catalysis. One possible proposal for this transition state appears in Chart 1 and shows the displacement of the zinc-bound water accompanied by formation of two proton bridges. If these are of the sort described by Kreevoy (Kreevoy et al., 1977), they will manifest themselves in transition-state fractionation factors that are less than unity and produce normal isotope effects.

Mechanistic Origins of Slow-Binding Inhibition of Metalloendoproteinases. In this paper, we suggest that the interaction of Ala[N]hPhe-Leu-anilide and SLN proceeds through a rate-limiting transition state that is characterized by ligand exchange on zinc with displacement of the zinc-bound water molecule to bulk solvent. The chemistry of this step rate-limits the association process and, thus, accounts for the magnitude of k_{on}, which is at least 10^3 times slower than the diffusion limit. This mechanism is supported not only by pH dependence and solvent isotope effect studies but also by a large enthalpy of activation for k_{on} of 12 kcal/mol. The generality of this mechanism is supported by the observation of similar isotope effects for the slow-binding inhibition of TLN by phosphoramidon (Izquierdo-Martin & Stein, 1992b) and the slow-binding inhibition of SLN by a peptide phosphonamidate (Izquierdo-Martin & Stein, 1992b, 1993). These values are summarized in Table 4 and show large normal solvent isotope effects for all three systems.

Two other mechanisms that are frequently used to explain slow-binding inhibition are a conformational change of an initially formed E–I complex and rare-form inhibition. A mechanism involving a rate-limiting conformational change has the same kinetic form as Scheme 2, but k_i would be rate-

[6] The term "rare-form inhibition" is equally valid for situations in which a thermodynamically rare form of the *inhibitor* combines with enzyme.

Table 4: Solvent Isotope Effects for the Association of Inhibitors with Stromelysin and Thermolysin

enzyme and inhibitor	pH	k_{on} (mM^{-1} s^{-1})	$^{D}k_{on}$
TLN and phosphoramidon	5.5	110 ± 12	1.70 ± 0.05
SLN and peptide phosphonamidate	5.0	3.4 ± 0.2	1.52 ± 0.10
	6.0	9.8 ± 0.3	1.51± 0.11
SLN and Ala[N]hPhe-Leu-anilide	5.5	41 ± 4	1.64 ± 0.07
	7.5	11 ± 1	1.81 ± 0.08

limited by conformational isomerization of E–I and not by chemistry. In rare-form inhibition, the only form of the enzyme that can combine with inhibitor is a thermodynamically unfavored or "rare" form.[6] While the association process still occurs at the diffusion limit, the experimentally observed value of k_{on} is diminished in proportion to the equilibrium constant governing the distribution of total enzyme. This is expressed in

$$k_{on,app} = \frac{k_{on}}{1 + K_{eq}} \quad (22)$$

where $K_{eq} = [E]/[E']$ and E′ is the rare form of the enzyme with which inhibitor can combine. If $K_{eq} = 10^3$, then $k_{on,app} = k_{on}/10^3$.

The experimental results reported herein, solvent isotope effects, activation energies, and pH dependencies, are inconsistent with these two mechanisms. Combined with other studies (Izquierdo-Martin & Stein, 1992b, 1993), these results suggest a mechanism for association that must involve rate-limiting chemistry.

ACKNOWLEDGMENT

We thank Dr. Karen Owens of the Medicinal Chemistry Department of Merck Research Laboratories for determining pK_a values of Ala[N]hPhe-Leu-anilide.

REFERENCES

Bardsley, W. G., Leff, P., Kavanagh, J., & Waight, R. D. (1980) *Biochem. J. 187*, 739–765.

Chapman, K. T., Kopka, I. E., Dutette, P. L., Esser, C. K., Lanza, T. J., Izquierdo-Martin, M., Niedzwiecki, L., Chang, B., Harrison, R. K., Kuo, D. W., Lin, T. Y., Stein, R. L., & Hagmann, W. K. (1993) *J. Med. Chem.* (in press).

Harrison, R., Teahan, J., & Stein, R. (1989) *Anal. Biochem. 180*, 110–113.

Harrison, R. K., Chang, B., Niedzwiccki, L., Stein, R. L. (1992) *Biochemistry 31*, 10757–10762.

Izquierdo-Martin, M., & Stein, R. L. (1992a) *J. Am. Chem. Soc. 114*, 325–331.

Izquierdo-Martin, M., & Stein, R. L. (1992b) *J. Am. Chem. Soc. 114*, 1527–1528.

Izquierdo-Martin, M., & Stein, R. L. (1993) *Bioorg. Med. Chem. 1*, 19–26.

Kassebaum, J. W., & Silverman, D. N. (1989) *J. Am. Chem. Soc. 111*, 2691–2696.

Knight, C. G., Willenbrock, F., & Murphy, G. (1992) *FEBS Lett. 296*, 263–266.

Kreevoy, M. M., Liang, T., & Chang, K. C. (1977) *J. Am. Chem. Soc. 99*, 5207–5209.

Kurz, L. C., Moix, L., Riley, M. C., & Frieden, C. (1992) *Biochemistry 31*, 39–48.

Lark, M. W., Saphos, C. A., Walakovits, L. A., & Moore, V. L. (1990a) *Biochem. Pharmacol. 39*, 2041–2049.

Lark, M. W., Walakovits, L. A., Shah, T. K., VanMiddlesworth, J., Cameron, P. M., & Lin, T.-Y. (1990b) *Connect. Tissue Res. 25*, 49–65.

Matrisian, L. M. (1990) *Trends Genet. 6*, 121–126.

Monsingo, A. F., & Matthews, B. W. (1984) *Biochemistry 23*, 5724–5729.

Morrison, J. F., & Walsh, C. T. (1988) *Adv. Enzymol. Relat. Areas Mol. Biol. 61*, 201–301.

Niedzwiecki, L., Teahan, J., Harrison, R., & Stein, R. L. (1992) *Biochemistry 31*, 12618–12623.

Netzel-Arnett, S., Mallya, S. K., Nagase, H., Birkedal-Hansen, H., & Van Wart, H. E. (1991) *Anal. Biochem. 195*, 86–92.

Quinn, D. M., & Sutton, L. D. (1991) *Enzyme Mechanism from Isotope Effects*, CRC Press, Boca Raton, FL.

Schmidt, J., Chen, J., DeTraglia, M., Minkel, D., & McFarland, J. T. (1979) *J. Am. Chem. Soc. 101*, 3634–3640.

Schowen, K. B., & Schowen, R. L. (1982) *Methods Enzymol. 87*, 551–606.

Shapiro, R., & Riordan, J. F. (1984) *Biochemistry 23*, 5234–5240.

Stack, M. S., & Gray, R. D. (1989) *J. Biol. Chem. 264*, 4277–4281.

Stein, R. L. (1985a) *J. Am. Chem. Soc. 107*, 7768–7769.

Stein, R. L. (1985b) *J. Am. Chem. Soc. 107*, 6039–6043.

Stein, R. L., & Matta, M. S. (1985) *Fed. Proc., Fed. Am. Soc. Exp. Biol. 44*, 1055.

Stein, R. L., Elrod, J. P., & Schowen, R. L. (1983) *J. Am. Chem. Soc. 105*, 2446–2452.

Stein, R. L., Strimpler, A. M., Hitoshi, H., & Powers, J. C. (1987) *Biochemistry 26*, 1305–1314.

Stein, R. L., & Izquierdo-Martin, M. (1993) *Arch. Biochem. Biophys.* (in press).

Teahan, J., Harrison, R., Izquierdo, M., & Stein, R. L. (1989) *Biochemistry 28*, 8497–8501.

Venkatasubban, K. S., & Schowen, R. L. (1985) *CRC Crit. Rev. Biochem. 17*, 1–41.

Whitman, S. E., Murphy, G., Angel, P., Rahmsdorf, H. J., Smith, B., Lyons, A., Harris, T. J. R., Herrlich, P., & Docherty, A. J. P. (1986) *Biochem. J. 240*, 913–916.